AIAA 94-2190
Noise Radiation by Instabilty Waves in
Coaxial Jets

M. Dahl
NASA-Lewis
Cleveland, OH
P. J. Morris
Penn State University
University Park, PA

25th AIAA Fluid Dynamics Conference

June 20-23, 1994 / Colorado Springs, CO

NOISE RADIATION BY INSTABILITY WAVES IN COAXIAL JETS

Milo Dahl*
NASA Lewis Research Center
Cleveland, OH 44135

Philip J. Morris†
Penn State University
University Park, PA 16802

ABSTRACT

In this paper predictions are made for the noise radiation from supersonic coaxial jets. The noise in the downstream arc of a supersonic jet is dominated by highly directional radiation from the supersonically convecting large scale structures in the jet mixing layer. Since the mean flow is not described easily in terms of simple analytic functions, a numerical prediction is made for its development. The compressible Reynolds-averaged boundary layer equations in cylindrical polar coordinates are solved. A mixing length turbulence model is used. Empirical correlations are developed for the effects of velocity and temperature ratio and Mach number. Both normal and inverted velocity profiles are considered. Comparisons with measurements for both single and coaxial jets show good agreement. The large scale structures are modeled as instability waves. The noise radiation generated by the instability waves is determined by a matching between the inner instability wave solution and the outer acoustic solution. Predictions are made for the differences between the noise radiated by coaxial jets with different operating conditions and a single equivalent jet with the same exit area, thrust, and mass-flow.

1 INTRODUCTION

The renewed interest in the creation of a High Speed Civil Transport that is economically viable and environmentally compatible has re-energized research efforts on supersonic jet noise. This noise issue was intensely addressed in the supersonic transport program during the 1960's. When the program was abruptly terminated in 1971, the large scale design effort stopped; however, a low level generic research program continued through the 1970's allowing small scale experiments and theoretical studies to advance the ideas that were beginning to appear. Given its history and the technical issues that remain to be addressed, the problem of community noise generated by supersonic jets is still a strong research motivator. To meet FAR 36 Stage 3 noise regu-

---

* Research Scientist
† Boeing Profesor of Aerospace Engineering, Associate Fellow AIAA

lations, noise suppression technology will need to be advanced beyond current levels. Thus, there is a continuing interest to understand the jet noise generation process, particularly those processes that are important in supersonic jet noise. This paper examines a method to modify the noise generation from a supersonic jet. A single, supersonic, axisymmetric jet with given initial velocity and temperature conditions is replaced by a dual stream, coaxial jet with different initial velocities and different initial temperatures. At least one of the jet streams is supersonic. For classification purposes, when the coaxial jet flow has a higher inner stream velocity than an outer stream velocity, the jet is referred to as a normal velocity profile (NVP) jet. If the outer stream velocity is higher than the inner stream, the jet has an inverted velocity profile (IVP). The study combines analytical and numerical techniques. The analytical technique is based on the theory that instability waves propagating in the jet shear layer at phase velocities that are supersonic relative to ambient are the dominant sources of mixing noise radiating in directions downstream of the jet. Shocks are not considered in this study; hence, the noises associated with them are ignored in the analysis. To complete the analytical solution, the developing mean flow properties must be known at every axial location. Due to the difficulties in the description of the development of normal and inverted profile jets with various operating conditions, the mean flow is determined numerically.

The interest in the measurement of the noise radiated by coaxial jets increased as the by-pass jet was introduced as an alternative propulsion system to the noisy turbojet engine. Early measurements for subsonic jets indicated that there could be noise benefits in the use of coaxial jets with normal velocity profiles. Using small scale nozzles, Dosanjh et al [1], [2] and Yu [3] observed, measured, and documented the existence of a minimum noise condition for shock containing coaxial jets. They found that when the outer nozzle pressure ratio was fixed above critical, the inner nozzle pressure ratio could be increased from no flow conditions to some point where the measured overall sound power level was a minimum, less than the outer jet alone. For higher inner pressure ratios, the noise increased. This minimum noise con-

dition always occurred for inner nozzle pressure ratios less than the outer nozzle pressure ratio indicating that the coaxial jet operated with an inverted velocity profile. The optical shadowgraphs showed that the outer stream repetitive shock structure was destroyed at the minimum noise condition and replaced by a composite shock structure just downstream of the nozzle exit. Hence, the overall noise reduction was primarily due to a decrease in shock associated noise. The minimum noise condition depended on nozzle geometry with inner nozzle pressure ratios varying from 2.22 to 2.63.

Further studies on a larger scale coaxial supersonic nozzle were conducted and the results are detailed by Ahuja [4], Bassiouni [5] and Bhutiani [6]. They confirmed the existence of a minimum noise condition and noted that downstream of the composite shock structure, the shocks were very weak or nonexistent indicating that the flow was similar to a properly expanded flow. Noise reductions were measured at all frequencies and at all angles. This would mean that not only was shock noise reduced, which dominates in the upstream direction, but that mixing noise was reduced as well, which dominates in the downstream direction. It was also found that directivity patterns could be changed by the choice of pressure and temperature operating conditions. Tanna [7] conducted measurements of shock-free coaxial jets with inverted velocity profiles to study the effects of profile shaping in jet mixing noise. In addition, care was taken in the choice of initial velocity and temperature conditions, as well as exit area, in order to compare results on a constant thrust, mass flow, and exit area basis to a fully mixed equivalent single jet or reference jet. They found that high frequencies increased at all angles and that low frequencies decreased at angles closer to the jet exit axis. These changes were relative to the reference jet and they became larger as the velocity ratio increased above unity. Far field spectra remained largely unchanged by higher temperature ratios for a coaxial jet with both velocities the same. Since the far field spectra were peaking at the lower frequencies, the overall sound pressure levels were quieter for $U_2/U_1 > 1$ at smaller angles and noisier at 90 degrees. The higher frequency noise was generated primarily from the outer shear layer before the streams merged. As U_2/U_1 increased, the outer shear layer had a larger velocity difference to ambient resulting in higher eddy convection velocities, higher source velocities, and more noise. Conversely, the lower frequency noise was generated downstream of merging where the velocities were lower, resulting in less noise. Similar results were measured by Maus [8]. They concluded that the rapid decay of the maximum mean velocity in inverted velocity profile jets was an important reason for noise reduction compared to the reference jet.

After examining shock-free, inverted profile coaxial jet data, Tanna [9] re-examined some of the normal velocity profile data and compared the results to a reference jet at the same thrust, mass flow, and exit area. His conclusion was that normal profile coaxial jets, with both inner stream velocity and temperature greater than the outer stream, are noisier than the reference jet. Given the constraint of constant exit area, one stream will always have a velocity higher than the reference jet in order to maintain constant total thrust and mass flow. Since the maximum velocity of a normal profile jet persists longer than the maximum velocity of an inverted profile jet then, in a Lighthill sense, the normal velocity profile jet would generate more noise than the inverted profile jet. The experimental work on coaxial jets was continued by Tanna et al [10] into the supersonic regime. The converging nozzles were operated above critical pressure ratios resulting in underexpanded, shock-containing jet flows. They also defined a minimum noise condition based on overall sound pressure level measurements at upstream angles where shock associated noise dominates. For a fixed outer nozzle pressure ratio above critical, minimum noise was found when the inner nozzle pressure ratio was slightly above critical at about 1.9. Depending on the initial velocities and temperatures of the two jet streams. this condition was found to hold for both inverted velocity profiles and normal velocity profiles.

Measurements from different nozzles at different conditions have provided data for empirical models, Stone [11], Stone [12] and Stone [13], and correlations, Pao [14]. A more theoretical approach based on turbulence modeling and Lighthill's independent noise producing eddies was proposed by Chen [15]. A turbulence model was used to calculate the mean flow properties that were the only quantities used for the acoustic calculations. A more elaborate theoretical model was proposed by Balsa and Gliebe [16] and Gliebe and Balsa [17]. They used turbulence modeling to predict both the mean flow and turbulence properties. With a model for the acoustic source of an elemental jet volume based on local turbulence properties, these results were used in Lilley's equation to predict far field radiated noise levels and spectra. Gliebe et al [18] recently summarized this model and made comparisons to various jet noise suppression nozzles. These models tend to agree favorably with measured data since they all contain factors that were derived from measured data.

In the present paper, we provide a model for the noise generation by the instability waves or large scale structures in a coaxial jet. The prediction of the development of the mean flow is described in the next section. Calculations for the evolution of instability waves in coaxial jets are presented next. The procedure for the calcu-

2

lation of their radiated noise is also given. Finally, a preliminary parametric study is conducted to compare the noise radiated by both NVP and IVP supersonic jets with a single equivalent jet with the same exit area, mass flow, and thrust.

2 MEAN FLOW DEVELOPMENT

This section discusses the methodology used to calculate the mean flow development of a compressible, coaxial jet. Both subsonic and supersonic conditions are calculated. When the jet exit conditions are supersonic, the jet static pressure is matched to the ambient pressure; hence, the flow is perfectly expanded. The approach is numerical with many simplifying assumptions used in the governing equations. These assumptions also lead to the need for a turbulence model to close the set of governing equations.

For the most part, in the past, the calculation of instability waves in a single axisymmetric jet have used analytic functions to characterize the mean flow. These analytic functions have been based on results from experimental measurements where data were correlated using local similarity variables. Michalke [19] summarized the use of different analytic functions in the calculation of instability waves. The measured data typically include only velocity profile results which are sufficient for incompressible instability wave calculations. When compressibility is important, the instability wave calculations require that either the temperature or the density profile be specified. Often, approximations have been made that allow the Crocco-Busemann relationship to be used. This defines the temperature or density profile to be a function of the velocity. Our calculations for both subsonic and supersonic single jets, using the procedure described below, show good agreement between the predicted density profiles and those obtained with Crocco's relationship. Detailed comparisons are given by Dahl [20].

When it comes to a coaxial jet, it is not clear how to derive appropriate analytic functions to describe the profiles at all axial locations. For a single supersonic jet, Tam and Burton [21] used a generalized half-Gaussian function to describe the mean velocity at all axial locations. The function parameters, centerline velocity, core radius, and half-width of the mixing region, were defined by cubic spline fits to measured data. The density profile was found by keeping the total temperature constant. This approach was possible due to the availability of measured data; however, there is little measured data for coaxial jets, especially with supersonic conditions, that would allow an analytical description to be made at all axial locations including the merging region of a normal profile and an inverted profile into

a single jet. Thus, the decision was made to generate mean profiles for the coaxial jets numerically. Morris [22] and Morris and Baltas [23] calculated instability waves using numerically generated velocity profiles for a single incompressible jet. The extension here is to include compressibility effects into the spreading and merging of a coaxial jet.

2.1 TURBULENCE MODEL

In the development of a prediction scheme for the mean properties of a coaxial jet, our emphasis has been on simplicity and robustness. Also, since the derivatives of the mean velocity and density must be evaluated accurately for the instability wave calculations, a very fine grid is necessary. This has led us to choose a simple turbulence model. Though this results in a high level of empiricism, the goals of efficiency, accuracy and robustness have been achieved.

The compressible equations of motion are simplified in the present case to their boundary layer form. The assumption is also made that density-velocity correlations may be neglected: the Morkovin-Bradshaw hypothesis. The Reynolds stress and heat flux terms are described by a mixing-length model, such that

$$ - \rho \overline{u'v'} = \mu_T \frac{\partial u}{\partial r} \tag{1} $$

and

$$ - \rho c_p \overline{v'T'} = \frac{c_p \mu_T}{\mathrm{Pr}_T} \frac{\partial T}{\partial r}. \tag{2} $$

with,

$$ \mu_T = \rho (C_1 C_2 \ell)^2 \left| \frac{\partial u}{\partial r} \right| \tag{3} $$

In eqn. (3) ℓ is a characteristic mixing length scale. The factor C_1 is the incompressible part of the mixing length constant. It depends on the velocity ratio $r = U_2/U_1$ and the density ratio $s = \rho_2/\rho_1$ between the two streams either side of the shear layer. Equations for the expected vorticity thickness growth rate have been developed by many investigators from experimental evidence. Thus, given that we know the vorticity thickness growth rate for a fixed r and s, we adjusted the C_1 factor (C_2 set to 1) until the calculated initial vorticity thickness growth rate of a single jet agreed with the predicted value. Continuing this process for a range of r and s values resulted in a series of calibration curves for C_1. A more detailed discussion is given by Dahl [20]. The C_2 factor is the compressible part of the mixing length constant. Its purpose is to decrease the growth of the shear layer as compressibility effects become important. It depends on a Mach number in a frame of reference convecting with the real phase speed of a growing disturbance in the

shear layer. This convected Mach number depends on r and s and on the Mach number of one of the streams. Experimentalists have used the convected Mach number to correlate the normalized measured growth rates of compressible shear layers. We developed an equation that fits through this correlated data in order to predict shear layer growth rates for given flow conditions. Thus, we proceeded to calibrate the C_2 factor given that C_1 is allowed to take on its previously calibrated value for the given r and s. C_2 was adjusted until the calculated initial vorticity thickness growth rate agreed with the predicted value. For this case, a single calibration curve was generated. Again, details are given by Dahl [20].

The characteristic length scale is related to the vorticity thickness. For example, in the NVP case,

$$\ell = \frac{\Delta U_{max}}{|\partial u/\partial r|_{max}} \qquad (4)$$

where ΔU_{max} is the largest ΔU between the two values determined by using the separation point. The separation point is located at the local minimum of $|\partial u/\partial r|$. The C_1 and C_2 factors are also determined from the edge conditions that gave us ΔU_{max}. The maximum gradient $|\partial u/\partial r|_{max}$ is the largest value of $|\partial u/\partial r|$ that occurs in the merging profile. This approach for determining C_1, C_2, and ℓ for a merging normal profile has the advantage that as the flow transitions into a single jet profile, the C_1, C_2, and ℓ factors transition into the appropriate form for a single jet.

In the IVP case, during merging, the local maximum in the velocity profile (where $\partial u/\partial r = 0$) is used to define the separation point between the two shear layers. As long as the inner core exists, the two merging shear layers are treated separately, but their mixing length constants are added as follows:

$$(C_1 C_2 \ell)_{total} = (C_1 C_2 \ell)_{inner} + (C_1 C_2 \ell)_{outer} \qquad (5)$$

This increases μ_T across the profile to mimic the increased turbulent action as the inverted profile starts to merge. When the inner core ends, eqn. (5) is no longer used and it is assumed that the mixing process in the outer shear layer dominates the flow, hence $(C_1 C_2 \ell)_{total} = (C_1 C_2 \ell)_{outer}$. As with the normal profile, this usage of C_1, C_2, and ℓ transitions into the proper usage for a single jet downstream. It should be noted that the mixing length model gives $\mu_T = 0$ at the local maximum, which is unrealistic. The simple solution taken here was to smooth the $|\partial u/\partial r|$ profile, and hence smooth μ_T. Further details of this process are given by Dahl [20].

2.2 NUMERICAL METHOD

In the present approach the equations of motion are transformed into stream function coordinates using,

$$r\rho u = \frac{\partial \Psi}{\partial r} \qquad \text{and} \qquad r\rho \tilde{v} = -\frac{\partial \Psi}{\partial x}. \qquad (6)$$

where $\tilde{v}$ is the mass averaged radial component of the mean velocity. The boundary layer equations may then be written,

$$\frac{\partial u}{\partial x} = \frac{\partial}{\partial \Psi}\left[r^2 \rho u \mu_{eff} \frac{\partial u}{\partial \Psi}\right] \qquad (7)$$

$$\frac{\partial H}{\partial x} = \frac{\partial}{\partial \Psi}\left[r^2 \rho u \frac{\mu_{eff}}{Pr_{eff}} \frac{\partial H}{\partial \Psi}\right] + \frac{\partial}{\partial \Psi}\left[r^2 \rho u^2 \left(\mu_{eff} - \frac{\mu_{eff}}{Pr_{eff}}\right)\frac{\partial u}{\partial \Psi}\right] \qquad (8)$$

where H is the mean enthalpy and,

$$\mu_{eff} = \mu + \mu_T \qquad (9)$$

and,

$$Pr_{eff} = \frac{1 + \frac{\mu_T}{\mu}}{\frac{1}{Pr} + \frac{1}{Pr_T}\frac{\mu_T}{\mu}} \qquad (10)$$

Equations (7) and (8) are the basis for the numerical work of Patankar and Spalding [24] and Crawford and Kays [25].

These equations can be differenced in a variety of ways; explicitly as in Madni and Pletcher [26], implicitly on an evenly spaced Ψ-grid as in Donovan and Todd [27], or transformed to a normalized Ψ-grid and implicitly differenced as in Patankar and Spalding [24]. Each of these numerical methods were found to have problems. The explicit DuFort-Frankel method [26], had stability problems. The implicit Crank-Nicolson method using an evenly spaced Ψ-grid [27] could not provide enough resolution at the outer low speed edges of the jet. Finally, Patankar and Spalding's method had problems with entrainment boundary conditions at the outer edge. Each of these problems were overcome by using fully implicit differencing and, what is considered to be, natural grid stretching and natural outer boundary entrainment. By choosing a fully implicit method, the numerical problem is inherently stable. The problem of grid resolution is solved by using an evenly spaced r-grid.

Details of the finite difference algorithm are given by Dahl [20]. The stream function is obtained from the axial velocity using the trapezoidal rule. Since the problem is axisymmetric a symmetry boundary condition is enforced at $r = 0$. The outer boundary condition is set such that the outer two boundary values equal the freestream values. The consequence of this boundary condition is that the jet flow, expanding due to mixing, must never reach the outer grid boundary. This problem is overcome by adding more grid points to the problem further

4

downstream. All variables are assigned their freestream values at the new grid points. As the shear layer of the jet expands, it becomes possible to increase the Δr-grid spacing since less grid points are necessary to define the shear layer accurately as was initially necessary for the thin shear layer. Thus, we do not simply continue to add grid points as the flow expands, but we can, from time to time, reduce the number of grid points by increasing the grid spacing. It was best to simply double the grid spacing so that the extrapolated guess for new variables occurred along constant grid lines in the x-direction. Thus, no interpolation was necessary.

2.3 MEAN FLOW PREDICTIONS

The prediction scheme was first tested on both subsonic and supersonic, heated and unheated, single jets and single jets in a moving stream. The agreement between the predictions and measurements were good. The details are given in Dahl [20]. In the high speed cases, the predictions were only as good as the empirical correlation for the effects of convective Mach number on the jet spreading rate. Since there is a moderate amount of scatter of the measured spreading rate data about this correlation, the predictions reflected these discrepancies.

Figure 1 shows a comparison between the predictions for a normal velocity profile coaxial jet and the measurements of Lau [28]. The jet operating conditions are, $u_1 = 411$ m/s, $T_1 = 657°$K; $u_2 = 274$ m/s, $T_2 = 292°$K; $r_1 = 1.96$ cm, $r_2 = 3.91$ cm. The agreement for the radial velocity profiles is good; however, the length of the potential core is underpredicted. This reflects the small differences between the correlation for the spreading rate and the measured value in this experiment. Figure 2 shows a comparison between the present predictions for an inverted velocity profile jet and the measurements of Lau [28]. The jet operating conditions are, $u_1 = 171$ m/s, $T_1 = 292°$K; $u_2 = 274$ m/s, $T_2 = 292°$K. Once again the agreement is good for the radial profiles and there is qualitative agreement for the centerline profiles. Additional comparisons have been made with experiments for both NVP and IVP jets. In all cases there is at least very good qualitative agreement and often good quantitative agreement. This provides us with confidence that the prediction scheme has met the goal of providing a robust and efficient method to describe the mean flow evolution in coaxial jets. These predictions have been used to determine the evolution of instability waves and their radiated noise. This analysis is described in the next section.
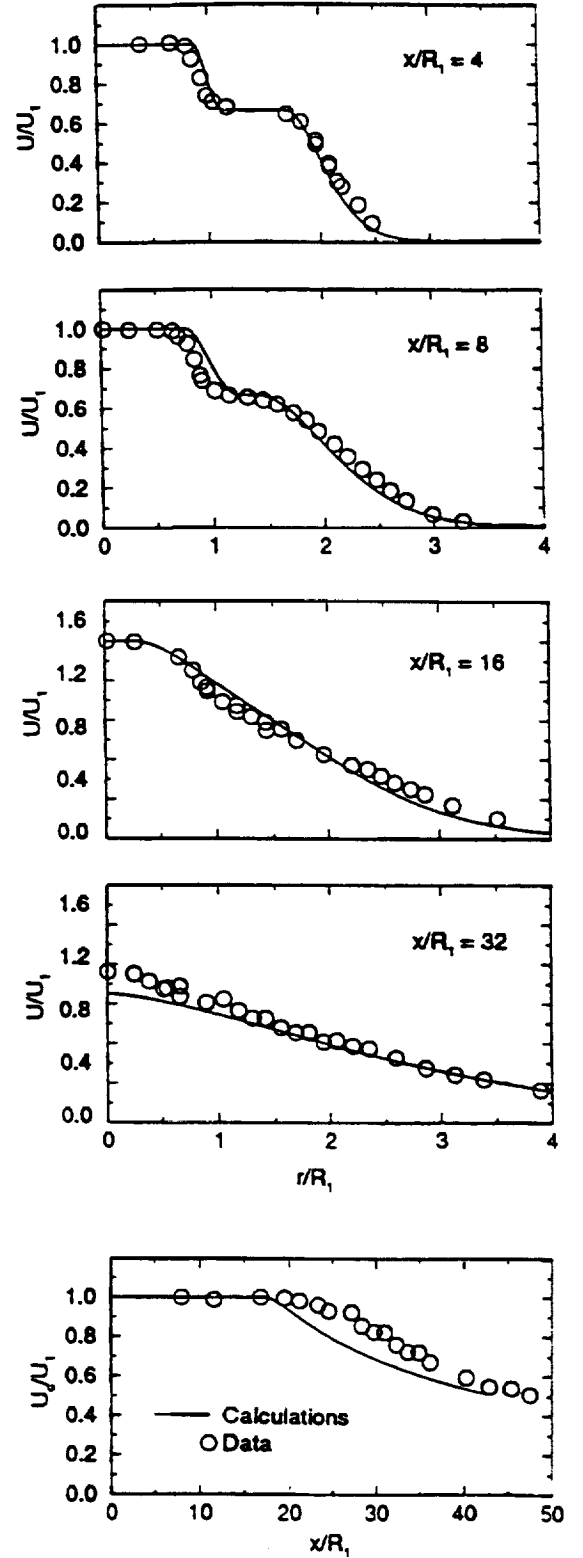

Figure 1 – Comparison of NVP predictions with measurements of Lau [28]
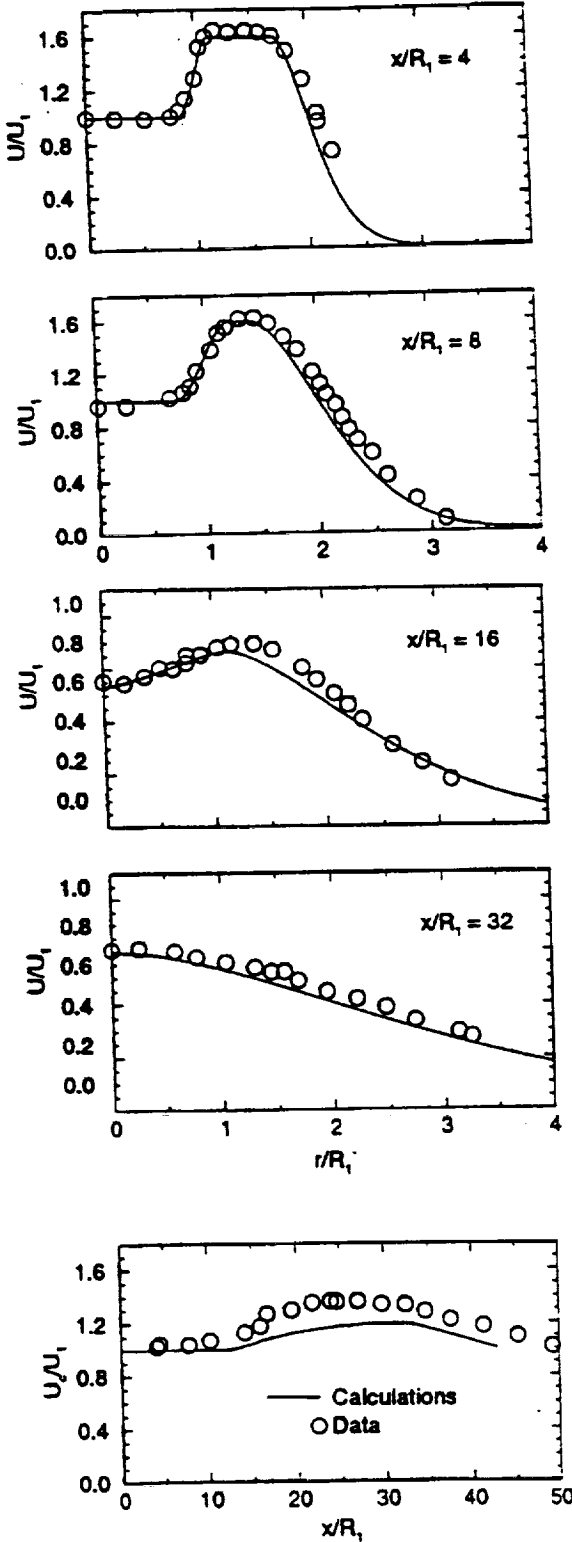
5

Figure 2 – Comparison of IVP predictions with measurements of Lau [28]

3 INSTABILITY WAVES AND RADIATED NOISE

This section describes the analysis that governs the development of the instability waves in these jets. The formulation follows the approach of Tam and Burton [21], with the addition of a nonzero free stream velocity. The analysis is given in detail by Dahl [20] and only a summary is given here.

The equations of motion for the fluctuations are the linearized, inviscid, compressible equations of continuity, momentum, and energy and the equation of state for a perfect gas. They are written in a polar cylindrical coordinate system (r, θ, x) with an origin at the center of the jet exit. It is recognized that the mean flow develops slowly in the axial direction. Thus, we transform the polar coordinates into an (r, θ, s) system where $s = \epsilon x$ and the mean velocity is given by,

$$\overline{\mathbf{V}} = (\epsilon \overline{v}_1(r, x), 0, \overline{u}(r, x)) \tag{11}$$

A series expansion in terms of ϵ is used to describe the fluctuations, with a fast periodic variation given by,

$$\exp\left[i\left(\frac{\phi(s)}{\epsilon} + n\theta - \omega t\right)\right] \tag{12}$$

Here, n is the azimuthal mode number, ω is the radian frequency and $\phi(s)$ is an axial phase function related to the axial wavenumber α by $d\phi/ds = \alpha(s)$. In general, the mth-order set of equations can be combined in favor of the pressure fluctuation $\hat{p}_m$ and cast in the form,

$$\frac{\partial^2 \hat{p}_m}{\partial r^2} + \left[\frac{1}{r} + \frac{2\alpha}{\overline{\omega}}\frac{\partial \overline{u}}{\partial r} - \frac{1}{\overline{\rho}}\frac{\partial \overline{\rho}}{\partial r}\right]\frac{\partial \hat{p}_m}{\partial r} + \left[\overline{\rho}M_j^2\overline{\omega}^2 - \frac{n^2}{r^2} - \alpha^2\right]\hat{p}_m = G_m(r, s) \tag{13}$$

where $\overline{\omega} = \omega - \alpha\overline{u}$. The right side term G_m depends on lower order terms only. To lowest order, $m = 0$, G_0 is zero and the equation is homogeneous. The homogeneous form of eqn. (13) is usually called the compressible Rayleigh Equation. The form of solution in the uniform flow outside the jet may be written,

$$\hat{p}_0 = A_0(s)H_n^{(1)}(i\lambda r) + B_0(s)H_n^{(2)}(i\lambda r) \tag{14}$$

The functions $H_n^{(1)}()$ and $H_n^{(2)}()$ are nth-order Hankel functions of the first and second kind, respectively, and

$$\lambda(\alpha) = \left[\alpha^2 - \overline{\rho}_\infty M_j^2\overline{\omega}_\infty^2\right]^{1/2} \tag{15}$$

The zeroth-order solution to eqn. (13) may be found by different methods and represents a homogeneous boundary value or eigenvalue problem. Here, we have used a finite-difference approximation to discretize the problem. In general, the solution may be written,

$$\hat{p}_0(r, s) = A_0(s)\zeta_1^p(r, s) + B_0(s)\zeta_2^p(r, s) \tag{16}$$

6

As $r \rightarrow \infty$, eqn. (16) must tend to eqn. (14) and as $r \rightarrow 0$, $\hat{p}_0$ must be finite.

In the region outside the jet, the ambient conditions $\bar{p}_\infty$ and $\bar{u}_\infty$ are uniform. Disturbances that travel in this region are independent of the coordinate system. Hence, distances traveled by the disturbance in any direction will be of the same scale. Using the cylindrical coordinate system of the inner solution, the axial coordinate was rescaled as $s = \varepsilon x$. To bring the radial coordinate in the outer region to the same scale, we let $\bar{r} = \varepsilon r$ be the scaled radial coordinate. The solution may be obtained by applying a Fourier transform in the s direction. The form of the solution for the Fourier transform of the axial velocity fluctuation may be written,

$$\tilde{u} = C y^{a/2} H_q^{(1)} \left(i \bar{k} y^{1/2} \right) \tag{17}$$

where,

$$y = \bar{r}^2 - \varepsilon^4 \bar{p}_\infty M_j^2 \bar{v}_\infty^2 \tag{18}$$

$$a = -i\varepsilon \bar{p}_\infty M_j^2 \bar{\omega}_k \bar{v}_\infty \tag{19}$$

$$\bar{k}^2 = \frac{1}{\varepsilon^2} \left(\varepsilon^2 k^2 - \bar{p}_\infty M_j^2 \bar{\omega}_k^2 \right) \tag{20}$$

$$q^2 = n^2 - \varepsilon^2 \bar{p}_\infty^2 M_j^4 \bar{\omega}_k^2 \bar{v}_\infty^2 \tag{21}$$

k is the transform variable in the s direction (an axial wavenumber) and $\bar{\omega}_k = \omega - \varepsilon k \bar{u}_\infty$. The unknown coefficients in the inner solution eqn. (15) and the outer solution eqn. (17) may be found by matching the two solutions in an overlap region. After considerable algebra it can be shown that, to lowest order in the near field,

$$p(r, \theta, x, t) = \int_{-\infty}^{\infty} g(\eta) H_n^{(1)}(i\lambda(\eta)r) e^{i\eta x} e^{in\theta} e^{-i\omega t} d\eta \tag{22}$$

where

$$g(\eta) = \frac{1}{2\pi} \int_{-\infty}^{\infty} \bar{A}_0(\varepsilon x) e^{i\phi(\varepsilon x)/\varepsilon} e^{-i\eta x} dx \tag{23}$$

with,

$$\lambda(\eta) = \left(\eta^2 - \bar{p}_\infty^2 M_j^2 \bar{\omega}_\eta^2 \right)^{1/2} \tag{24}$$

and $\bar{\omega}_\eta = \omega - \eta \bar{u}_\infty$.

The pressure in the far field may be obtained by rewriting the outer solution in spherical polar coordinates $x = R \cos \psi$ and $r = R \sin \psi$. The integral expression for the far field pressure may be approximated with the method of stationary phase. The stationary point is given by

$$\eta = \bar{\eta} = \frac{\bar{p}_\infty^{1/2} M_j \omega \cos \psi}{(1 - M_\infty^2)(1 - M_\infty^2 \sin^2 \psi)^{1/2}} - \frac{\bar{p}_\infty M_j^2 \bar{u}_\infty \omega}{1 - M_\infty^2} \tag{25}$$

and the sound power radiated per unit solid angle, the directivity, is given by,

$$D(\psi) = \frac{1}{2} |p|^2 R^2 = 2 \frac{|g(\bar{\eta})|^2}{[1 - M_\infty^2 \sin^2 \psi]} \tag{26}$$

Since the rate of spread of the jet is slow for the high speed jet and ϵ is very small the value of $\bar{A}_0(\varepsilon x)$ in eqn. (23) is taken to be a constant. In addition, $\phi(\varepsilon x)/\varepsilon = \int_0^x \alpha(x)\,dx$ where $\alpha(x)$ is the eigenvalue found from the local solution of the compressible Rayleigh equation. Thus to complete the solution it only remains to solve this equation at each axial location, use these results to obtain the axial wavenumber spectrum of the instability wave, eqn. (23), and then to obtain either the near field or far field from eqns. (22) or (26) respectively. Details of the numerical implementation are given by Dahl [20] and will be reported elsewhere. In the next section we validate our approach by comparisons with previous single jet analytic predictions and measurements. Predictions are then made for both NVP and IVP coaxial jets.

4 JET NOISE PREDICTIONS
4.1 SINGLE CIRCULAR JETS

We have compared our predictions with measured flow and acoustic data for single axisymmetric jets. One example is shown here. Further examples are given Dahl [20]. Seiner and Ponton [29] made measurements in a Mach 2.0 unheated jet. Our predictions for the mean flow development slightly underpredict the mixing rate at this Mach number and the length of the potential core is slightly overpredicted. However, the general flow development is represented qualitatively well. Figure 3 shows a comparison between the measured and predicted near field pressure contours for a Strouhal number, $St = 0.4$. The predictions are made to within an unknown constant, the initial amplitude of the instability wave, and the levels should be viewed in a relative sense. The directionality of the near field is captured well as is the axial location of the peak pressure fluctuations. Figure 4 shows the prediction and measurements for the far field directivity for $St = 0.2$. Once again the agreement is good. At higher angles to the jet axis, greater than 45° for these operating conditions, the measured levels level off and are higher than the predictions. This is because for these larger angles the noise is related to other generation mechanisms not included in the present predictions. These could include some weak shock-associated noise or other mixing noise sources. It should be emphasized that the present predictions do not rely on the measured mean velocity and

7

temperature profiles as the basis for the instability wave noise predictions. The calculations only rely on the operating conditions at the jet exit. Thus, we beleive that this calculation alone represents a significant advance in supersonic jet noise prediction capability over existing methods. In the next section the prediction scheme is applied to supersonic coaxial jets.

4.2 COAXIAL CIRCULAR JETS

In this section we conduct a limited parametric study of the noise radiation from coaxial, perfectly-expanded, supersonic jets. To cover a complete range of changes in all possible parameters represents an enormous task. Here we simply compare the effects of changing the operating conditions of both NVP and IVP jets to maintain the same thrust, mass-flow and exit area as a single equivalent jet (SEJ). The SEJ has operating conditions, exit velocity of 1330 m/s and exit temperature 1100 K. These exit conditions are appropriate for projected supersonic jet transport aircraft. With the exit area fixed, the NVP calculations have been conducted for a limited range of conditions and the IVP jets are operated at the minimum noise condition given by Tanna et al [10]. The area ratio is fixed at 1.25 and the external velocity is negligible. The procedures for the calculation of the exit conditions is given by Dahl [20]. The values chosen for the present study are shown in Table. 1.

4.2.1 NORMAL VELOCITY PROFILE JETS

The mean flow prediction scheme has been used to determine the development of the mean velocity and density. The end of the inner potential core increased with velocity ratio and decreased with inner jet temperature. The outer potential core length increases with outer jet velocity and lower outer jet temperatures. Predictions of the development of the instability waves on both the inner and outer jet shear layers have been made. These results have been used to determine their wavenumber spectra and the resulting near and far field pressure levels. Only a few summary results are given here for the far field directivities. Typical predictions are shown in figs. 5 and 6 for a Strouhal number 0.12 and a helical $n = 1$, and axisymmetric $n = 0$, mode respectively. Generally, for the helical mode, the relative levels for the coaxial jet are lower than the reference jet. Only the levels for the instability wave that generates the greatest far field levels have been included. This could be an instability wave associated with either the inner or outer jet shear layer. In general, as the density ratio $s = \rho_2/\rho_1$ decreases the inner high speed stream cools and the instability wave growth is enhanced on the inner shear layer and tends to dominate the radiated noise. For the axisymmetric mode the radiated noise is generally dominated by the
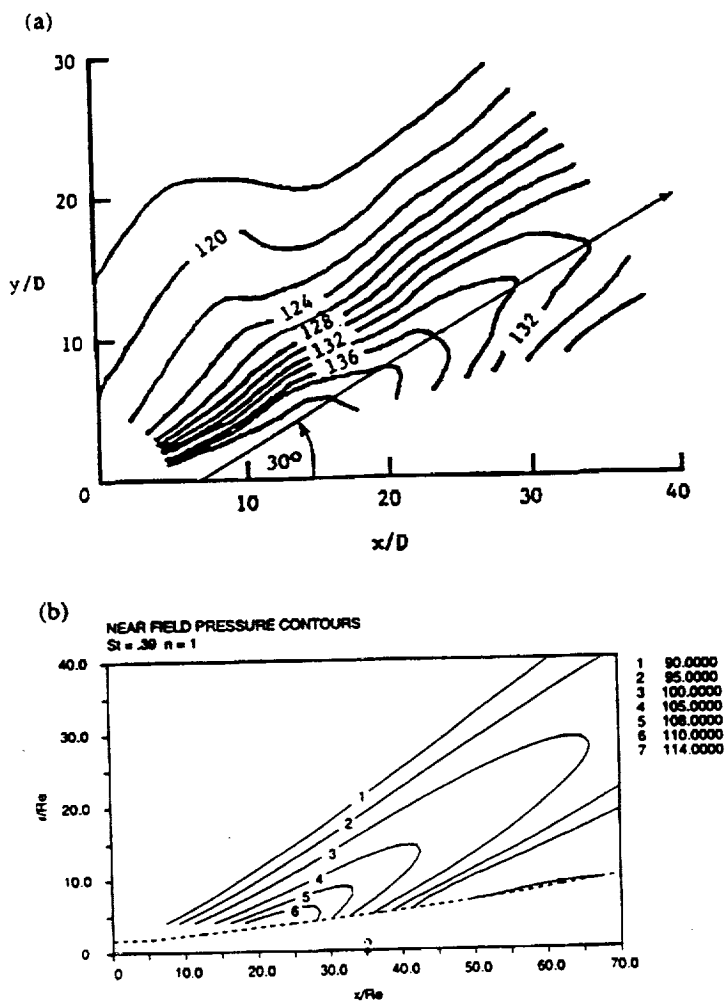

Figure 3 – Comparison of near field pressure contour predictions with measurements of Seiner and Ponton [29].
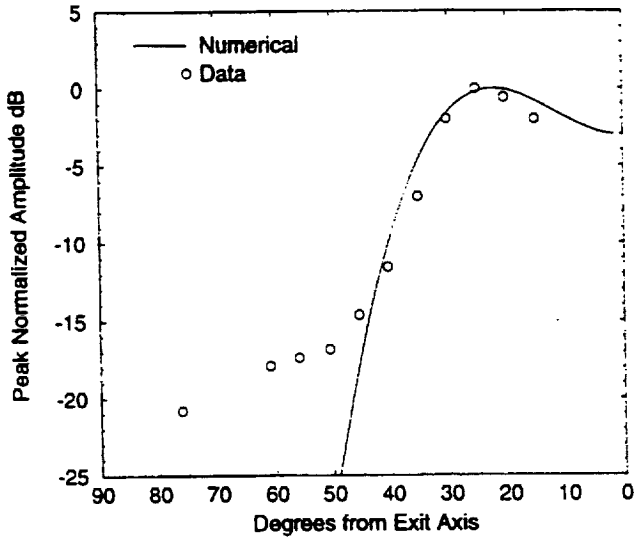
8

Figure 4 – Comparison of predicted far field directivity with measurements of Seiner and Ponton [29]

Figure 5 – Far field directivity patterns for NVP cases. $St = 0.12$, $n = 1$.

inner shear layer instability. However, the helical modes are generating higher noise levels in the far field. Also, the radiated noise levels may be either higher or lower than the SEJ. We note that for the NVP jets only the $r = u_2/u_1 = 0.8$, $s = 1.0$ and $r = 0.8$, $s = 2.0$ cases give reductions for both the axisymmetric and helical modes at all frequencies. Tanna [9] commented that the shock free NVP jet could be quieter than the SEJ for r close to unity and $s < 1$. Support for this conjecture appears in the $r = 0.8$, $s = 0.5$ case where reductions of nearly 10dB are predicted for the helical mode. There are some slight gains for the axisymmetric mode but the predicted far field levels for this mode are lower.

4.2.2 INVERTED VELOCITY PROFILE JETS

The extensive experimental studies by Dosanjh *et al* [1], [2] and Tanna *et al* [10] have shown the benefits in shock-associated noise production by operating at the minimum noise condition. Here, we consider the mixing noise from IVP jets operating on-design. The operating conditions chosen are given in Table 1. The mean flow predictions show a flow development similar to that measured by Au and Ko [30] for subsonic jets. As the two shear layers merge a local maximum in the axial velocity develops which moves towards the jet axis downstream. For the given operating conditions, that results in fixed Mach numbers for the inner and outer streams, as r increases and the temperatures adjust accordingly both potential
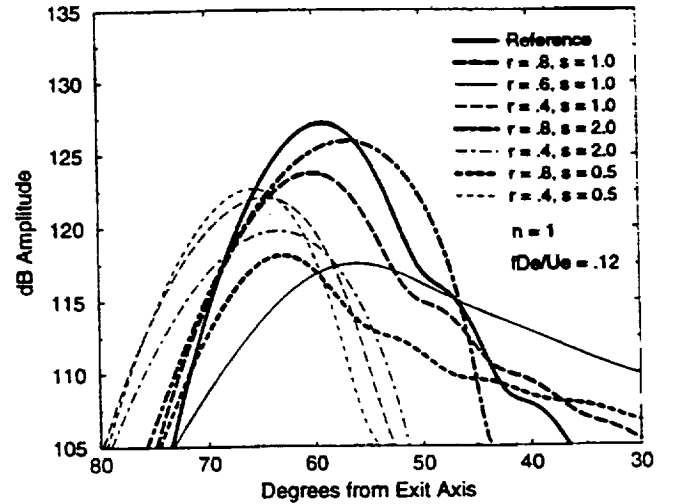

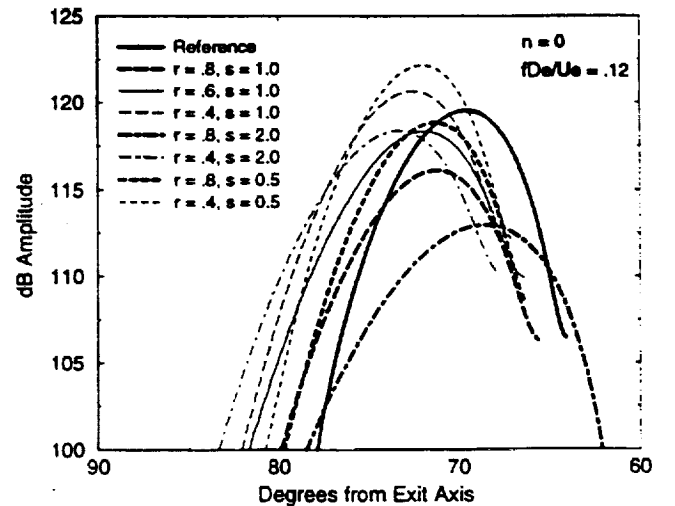Figure 6 – Far field directivity patterns for NVP cases. $St = 0.12$, $n = 0$.

Figure 7 – Far field directivity patterns for IVP cases. $St = 0.20$, $n = 1$.
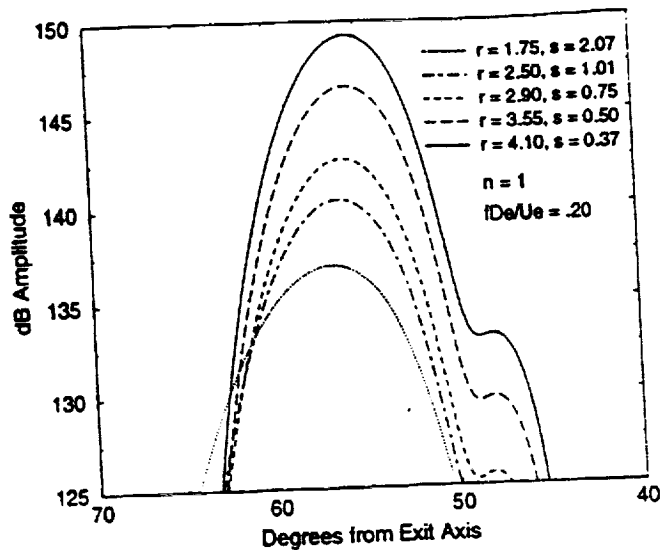

Figure 8 – Far field directivity patterns for IVP cases. $St = 0.20$, $n = 0$.

cores decrease in length. The location of the maximum velocity on the jet axis moves further downstream as the outer stream velocity increases. Figures 7 and 8 show the predicted far field directivities for $St = 0.2$ and the helical and axisymmetric modes respectively. A comparison with figs. 5 and 6 shows that the predicted levels are all higher than the SEJ. Tanna [9] concluded that shock-free IVP were noisier than the SEJ at high frequencies and quieter at low frequencies. We have found no evidence of this trend in these predictions. However, the minimum noise condition constraint has fixed the density ratio for a given area ratio. If there is to be any benefit to having a different s at the same value of r , the area ratio needs to be changed.

As a final calculation, we considered a change in the area ratio from 1.25 to 0.5. The value of r was fixed at 4.1, so that, for fixed thrust and mass flow the density ratio is increased from 0.37 to 0.59 and the outer stream Mach number increases to 3.2. This case was chosen for comparison as it produced the highest far field levels of any IVP case. Figure 9 shows the predicted far field directivities for the $St = 0.4$ and the helical mode. The peak levels are reduced by a decrease in the area ratio. Even though the outer stream has a higher initial velocity, its smaller thickness translates into a shorter outer potential core and increased spreading when the shear layers merge. This results in a faster decrease to the growth rates of the outer shear layer instability wave
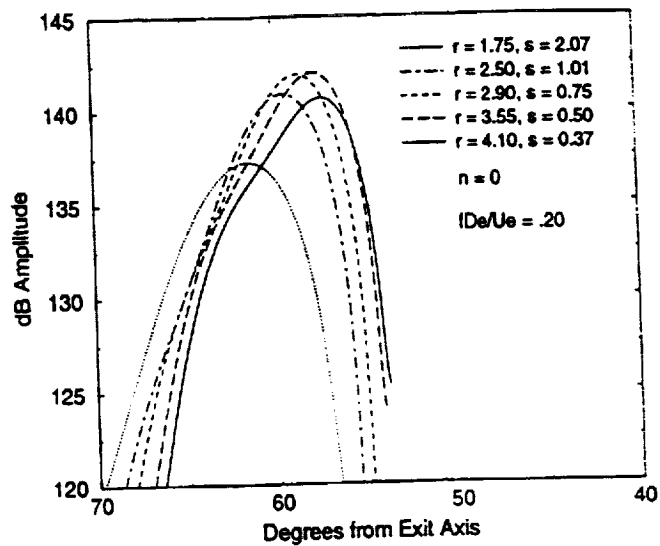
and a resulting lower far field level. Thus there are some benefits to operating with a lower area ratio.

5 SUMMARY

In this paper we have described the development of a procedure for the prediction of noise from the instability waves of supersonic coaxial jets. The development of the mean flow is predicted from a solution of the boundary layer equations and a simple, calibrated turbulence model. The evolution of the instability waves on the inner and outer shear layers are determined from a local solution of the compressible Rayleigh equation. The near and far field pressure levels are found by matching the instability wave solution with the outer acoustic solution.

The procedure developed in this paper enables predictions of relative levels in the near and far fields to be determined from knowledge only of the jet exit conditions. This represents a considerable advance over previous prediction schemes and offers the opportunity for efficient parametric studies to be conducted. In the present paper a limited study has been performed. The results indicate that, for a fixed area ratio, there are benefits from the use of a NVP jet compared to the SEJ. No such benefits accrued for IVP jets. However, changes in the area ratio could provide benefits in the IVP case.
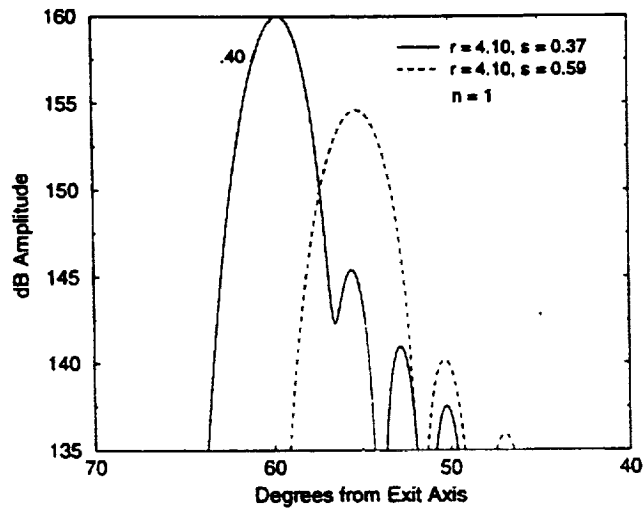
10

Figure 9 – Effect of area ratio on far field directivity patterns for IVP jet. $St = 0.40$, $n = 1$.

	r	s	U1(m/s)	U2(m/s)	T1(K)	T2(K)	M1	M2
Reference	–	–	1330.0	–	1100.0	–	2.0	–
Normal								
Case #								
2	0.80	1.00	1477.8	1182.2	1086.4	1086.4	2.2	1.8
3	0.60	1.00	1605.2	963.1	1032.6	1032.6	2.5	1.5
4	0.40	1.00	1662.2	665.0	916.7	916.7	2.7	1.1
5	0.80	2.00	1534.6	1227.7	1692.3	846.2	1.9	2.1
6	0.40	2.00	1900.0	760.0	1396.8	698.4	2.5	1.4
7	0.80	0.50	1425.0	1140.0	785.7	1571.4	2.5	1.4
8	0.40	0.50	1511.4	604.5	694.4	1388.9	2.9	0.8
Inverted								
Case #								
24	1.75	2.07	823.7	1441.4	1678.4	808.1	1.0	2.5
20	2.50	1.01	621.1	1552.9	954.5	937.9	1.0	2.5
21	2.90	0.75	556.0	1612.3	764.7	1011.0	1.0	2.5
22	3.55	0.50	·481.4	1708.9	573.3	1135.8	1.0	2.5
23	4.10	0.37	436.7	1790.6	471.9	1247.0	1.0	2.5

Table 1 Operating conditions for NVP and IVP jets and SEJ. Radius Ratio $r_2/r_1 = 1.5$; Velocity Ratio, $r = u_2/u_1 T$; Density Ratio, $s = \rho_2/\rho_1 = T_1/T_2$. (Constant Thrust and Constant Mass Flow).

REFERENCES

[1] Dosanjh, D. S., Abdelhamid, A. N. and Yu, J. C., "Noise Reduction from Interacting Coaxial Supersonic Jet Flows", *NASA SP*-207, 1969, pp. 63-101.

[2] Dosanjh, D. S.,Yu, J. C. and Abdelhamid, A. N., "Reduction of Noise from Supersonic Jet Flows", *A.I.A.A. Paper No.* 70-236, 1970.

[3] Yu, J. C. and Dosanjh, D. S., "Noise Field of Coaxial Interacting Supersonic Jet Flows", *A.I.A.A.Paper No.* 71-152, 1971

[4] Ahuja, K. K., "Noise Studies of Cold and Heated Model Jets at Supersonic and High Subsonic Speeds with Particular Reference to Noise Reduction," Ph.D. thesis, Syracuse University, 1976.

[5] Bassiouni, M. R., "Acoustic and Flow Characteristics of Cold High-Speed Coaxial Jets," Ph. D. thesis, Syracuse University, 1976.

[6] Bhutiani, P. K., "Investigations of the Radiated Noise from Coaxial Supersonic Jets to Study: I. The Effect of Heating One of the Jets. II. The Role of Lip Thickness on Noise Suppression," Ph.D. thesis, Syracuse University, 1976.

[7] Tanna, H. K., Tester, B. J. and Lau, J. C., "The Noise and Flow Characteristics of Inverted-Profile Coannular Jets," *NASA CR*-158995, 1979.

[8] Maus, J. R., Goethert, B. H. and Sundaram, C. V., "Noise Characteristics of Coannular Flows with Conventional and Inverted Velocity Profiles," *A.I.A.A. Paper No.* 80-0167, 1980.

[9] Tanna, H. K., "Coannular Jets – Are They Really Quiet and Why?" *J. Sound Vib.*, 72, 1980, pp. 97-118.

[10] Tanna, H. K., Brown, W. H. and Tam, C. K. W., "Shock Associated Noise of Inverted-Profile Coannular Jets, Part I: Experiments," J. Sound Vib., 98, 1985, pp. 95-113.

[11] Stone, J. R., "An Empirical Model for Inverted-Velocity-Profile Jet Noise Prediction," *NASA TM*-73838, 1977.

[12] Stone, J. R., Goodykoontz, J. H. and Gutierrez, O. A., "Effects of Geometric and Flow-Field Variables on Inverted-Velocity- Profile Coaxial Jet Noise and Source Contributions," *NASA TM*-79095, 1979.

[13] Stone, J. R., Groesbeck, D. E. and Zola, C. L., "Conventional Profile Coaxial Jet Noise Prediction," *AIAA Journal*, 21, 1983, pp. 336-342.

[14] Pao, S. P., "A Correlation of Mixing Noise from Coannular Jets with Inverted Flow Profiles," *NASA TP*-1301, 1979.

[15] Chen, C. Y., "A Model for Predicting Aero-Acoustic Characteristics of Coaxial Jets," *A.I.A.A. Paper No.* 76-4, 1976.

[16] Balsa, T. F. and Gliebe, P. R., "Aerodynamics and Noise of Coaxial Jets," *AIAA Journal*, 15, 1977, pp. 1550-1558.

[17] Gliebe, P. R. and Balsa, T. F., "Aeroacoustics of Axisymmetric Single- and Dual-Flow Exhaust Nozzles," *J. Aircraft*, 15, 1978, pp. 743-749.

[18] Gliebe, P. R., Brausch, J. F., Majjigi, R. K. and Lee, R., "Jet Noise Suppression," in *Aeroacoustics of Flight Vehicles: Theory and Practice. Volume 2: Noise Control*, NASA RP-1258, 1991.

[19] Michalke, A., "Survey of Jet Instability Theory," *Prog. Aerospace Sci.*, 21, 1984, pp. 159-199.

[20] Dahl, M., "The Aeroacoustics of Supersonic Coaxial Jets," Ph. D. thesis, Penn State University, 1994.

[21] Tam, C. K. W. and Burton, D. E., "Sound Generated by Instability Waves of Supersonic Flows. Part 2. Axisymmetric Jets," *J. Fluid Mechanics*, 138, 1984, pp. 273-295.

[22] Morris, P. J., "A Model for Broadband Jet Noise Amplification," *A.I.A.A. Paper No.* 80-1004, 1980.

[23] Morris, P. J. and Baltas, C., "Turbulence in Sound Excited Jets: Measurements and Theory," *A.I.A.A. Paper No.* 81-0058, 1981.

[24] Patankar, S. V. and Spalding, D. B., *Heat and Mass Transfer in Boundary Layers*, 2nd. edition, Intertext, London, 1970.

[25] Crawford, M. E. and Kays, W. M., "STAN5 - A Program for Numerical Computation of Two-Dimensional Internal and External Boundary Layer Flows," *NASA CR*-2742, 1976.

[26] Madni, I. K. and Pletcher, R. H., "Prediction of Turbulent Jets in Coflowing and Quiescent Ambients," *J. of Fluids Eng.*, 97, 1975, pp. 558-567.

[27] Donovan, L. F. and Todd, C. A., "Computer Program for Calculating Isothermal, Turbulent Jet Mixing of Two Gases," *NASA TN D*-4378, 1967.

[28] Lau, J. C., "A Study of the Structure of the Coannular Jet," *Lockheed Report* LG80ER0017, 1980.

12

[29] Seiner, J. M. and Ponton, M. K., "Aeroacoustic Data for High Reynolds Number Supersonic Axisymmetric Jets," *NASA TM*-86296, 1985.

[30] Au, H. and Ko, N. W. M., "Coaxial Jets of Different Mean Velocity Ratios, Part 2," *J. Sound Vib.*, **116**, 1987, pp. 427-443.

REPORT DOCUMENTATION PAGE

Public reporting burden for this collection of information is estimated to average 1 hour per response, including the time for reviewing instructions, searching existing data sources, gathering and maintaining the data needed, and completing and reviewing the collection of information. Send comments regarding this burden estimate or any other aspect of this collection of information, including suggestions for reducing this burden, to Washington Headquarters Services, Directorate for Information Operations and Reports, 1215 Jefferson Davis Highway, Suite 1204, Arlington, VA 22202-4302, and to the Office of Management and Budget, Paperwork Reduction Project (0704-0188), Washington, DC 20503.

1. AGENCY USE ONLY (Leave blank)	2. REPORT DATE	3. REPORT TYPE AND DATES COVERED
	Date 1994	Technical Memorandum

4. TITLE AND SUBTITLE
Noise Radiation by Instability Waves in Coaxial Jets

5. FUNDING NUMBERS
WU–505–62–52

6. AUTHOR(S)
Milo D. Dahl and Philip J. Morris

7. PERFORMING ORGANIZATION NAME(S) AND ADDRESS(ES)

National Aeronautics and Space Administration
Lewis Research Center
Cleveland, Ohio 44135–3191

8. PERFORMING ORGANIZATION REPORT NUMBER

E–9141

9. SPONSORING/MONITORING AGENCY NAME(S) AND ADDRESS(ES)

National Aeronautics and Space Administration
Washington, D.C. 20546–0001

10. SPONSORING/MONITORING AGENCY REPORT NUMBER

NASA TM–106738

11. SUPPLEMENTARY NOTES
Prepared for the 25th Fluid Dynamics Conference sponsored by the American Institute of Aeronautics and Astronautics, Colorado Springs, Colorado, June 20–23, 1994. Milo D. Dahl, Lewis Research Center and Philip J. Morris, Pennsylvania State University, University Park, Pennsylvania 16802. Responsible person, Milo D. Dahl, organization code 2660, (216) 433–3578.

12a. DISTRIBUTION/AVAILABILITY STATEMENT

Unclassified - Unlimited
Subject Category 71

12b. DISTRIBUTION CODE

13. ABSTRACT (Maximum 200 words)
In this paper predictions are made for the noise radiation from supersonic coaxial jets. The noise in the downstream arc of a supersonic jet is dominated by highly directional radiation from the supersonically convecting large scale structures in the jet mixing layer. Since the mean flow is not described easily in terms of simple analytic functions, a numerical prediction is made for its development. The compressible Reynolds-averaged boundary layer equations in cylindrical polar coordinates are solved. A mixing length turbulence model is used. Empirical correlations are developed the effects of velocity and temperature ratio and Mach number. Both normal and inverted velocity profiles are considered. Comparisons with measurements for both single and coaxial jets show good agreement. The large scale structures are modeled as instability waves. The noise radiation generated by the instability waves is determined by a matching between the inner instability wave solution and the outer acoustic solution. Predictions are made for the differences between the noise radiated by coaxial jets with different operating conditions and a single equivalent jet with the same exit area, thrust, and mass-flow.

14. SUBJECT TERMS
Supersonic coaxial jets; Noise radiation; Instability waves; Mean flow prediction; Noise prediction

15. NUMBER OF PAGES
16

16. PRICE CODE
A03

17. SECURITY CLASSIFICATION OF REPORT	18. SECURITY CLASSIFICATION OF THIS PAGE	19. SECURITY CLASSIFICATION OF ABSTRACT	20. LIMITATION OF ABSTRACT
Unclassified	Unclassified	Unclassified	

NSN 7540-01-280-5500